

Nitric Oxide Oxidatively Nitrosylates Ni(I) and Cu(I) C-Organonitroso Adducts

Stefan Wiese, Pooja Kapoor, Kamille D. Williams, and Timothy H. Warren*

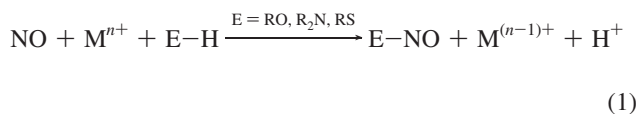
Department of Chemistry, Georgetown University, Box 571227, Washington, D.C. 20057-1227

Received May 1, 2009; Revised Manuscript Received September 23, 2009; E-mail: thw@georgetown.edu

Abstract: Monovalent nickel and copper β -diketiminato complexes react with $\text{ArN}=\text{O}$ ($\text{Ar} = 3,5\text{-Me}_2\text{C}_6\text{H}_3$, Ph) to give C-nitroso adducts that exhibit three different modes of bonding with varying degrees of N–O bond activation. The addition of ArNO to 2 equiv of $[\text{Me}_2\text{NN}]\text{Ni}(2,4\text{-lutidine})$ $\{[\text{Me}_2\text{NN}]^- = 2,4\text{-bis}(2,6\text{-dimethylphenylimido})\text{pentyl}\}$ gives $\{[\text{Me}_2\text{NN}]\text{Ni}\}_2(\mu\text{-}\eta^2\text{:}\eta^2\text{-ONAr})$ (**1a** and **1b**), which exhibit symmetrical bonding of the $\text{ArN}=\text{O}$ moiety between two $[\text{Me}_2\text{NN}]\text{Ni}$ fragments, with a N–O bond distance of 1.440(4) Å in **1a** that is significantly longer than those in free C-organonitroso compounds (1.13–1.29 Å). $[\text{Me}_2\text{NN}]\text{Cu}(\text{NCMe})$ reacts with 0.5 equiv of ArNO in ether to give the dinuclear adducts $\{[\text{Me}_2\text{NN}]\text{Cu}\}_2(\mu\text{-}\eta^2\text{:}\eta^1\text{-ONAr})$ (**2a** and **2b**), which exhibit η^2 and η^1 bonding of the $\text{ArN}=\text{O}$ moiety with separate $[\text{Me}_2\text{NN}]\text{Cu}$ fragments possessing N–O distances of 1.375(6) Å (**2a**) and 1.368(2) Å (**2b**). In arene solvents, one β -diketiminatocopper(I) fragment dissociates from **2** to give $[\text{Me}_2\text{NN}]\text{Cu}(\eta^2\text{-ONAr})$ (**3a** and **3b**), which may be isolated by the addition of 1 equiv of ArNO to $[\text{Me}_2\text{NN}]\text{Cu}(\text{NCMe})$. The X-ray structures of **3a** and **3b** are similar to those of related Cu(I) alkene adducts, with N–O distances in the narrow range 1.333(4)–1.338(5) Å. IR spectra of the nitrosobenzene adducts **1b**, **2b**, and **3b** exhibit ν_{NO} stretching frequencies at 915, 1040, and 1113 cm^{-1} , respectively, following the decreasing degree of N=O activation observed in the X-ray structures of species **1**, **2**, and **3**. Both **1a** and **3a** react with anaerobic $\text{NO}(\text{g})$ to give the corresponding N-aryl-N-nitrosohydroxylaminato complexes $[\text{Me}_2\text{NN}]\text{M}(\kappa^2\text{-O}_2\text{N}_2\text{Ar})$ [$\text{M} = \text{Ni}$ (**4**), Cu (**5**)]. In the reaction of dinuclear **1a** with NO , one $[\text{Me}_2\text{NN}]\text{Ni}$ fragment is trapped as the nickel nitrosyl $[\text{Me}_2\text{NN}]\text{Ni}(\text{NO})$. Reaction of the monovalent complex $[\text{Me}_2\text{NN}]\text{Cu}(\eta^2\text{-ONAr})$ with $\text{NO}(\text{g})$ to give divalent $[\text{Me}_2\text{NN}]\text{Cu}(\kappa^2\text{-O}_2\text{N}_2\text{Ar})$ represents an example of oxidative nitrosylation.

Introduction

Nitric oxide (NO) has a rich biochemistry with metalloenzymes, though targets for NO incorporation are not limited to the metal centers themselves.¹ For instance, copper ions are required to induce the S-nitrosylation of the two Cys β 93 residues of oxyhemoglobin with NO;² oxyhemoglobin exhibits a higher affinity for NO than its deoxy form.³ Redox-active metal ions may assist in the nitrosylation of organic substrates such as alcohols, amines, and thiols (eq 1):⁴



In such reductive nitrosylation reactions, nitric oxide is formally oxidized to NO^+ by the metal ion, which is reduced by one electron.

There are relatively few well-defined examples in which nitric oxide functionalizes a ligand within the coordination sphere of a metal. For instance, Ford demonstrated an intramolecular reductive nitrosylation at Cu^{2+} that results in N–NO bond formation at a bound tetraamine cyclam.⁵ Bergman mechanistically studied C–NO bond formation in the ligand-induced migratory insertion of $\text{Cp}^*\text{Co}(\text{NO})(\text{R})$ into $\text{Cp}^*\text{Co}(\text{N}(\text{O})\text{R})\text{PR}'_3$ ($\text{R} = \text{Me}, \text{Et}$).⁶ This behavior may be contrasted with double NO insertion into metal alkyls M-R to give N-alkyl-N-nitrosohydroxylaminato species $\text{M}(\kappa^2\text{-O}_2\text{N}_2\text{R})$.⁷ On the other hand, addition of nitrosonium (NO^+) to C-organonitroso adducts $[\text{Pt}(\text{ArNO})(\text{PPh}_3)_2]$ ($\text{Ar} = \text{Ph}, o\text{-MeC}_6\text{H}_4$) gave the diazeniumdiolate cations $\{[\text{Pt}(\kappa^2\text{-O}_2\text{N}_2\text{Ar})(\text{PPh}_3)_2]^+\}$.⁸

In biological environments, C-nitroso compounds RNO are known to form via the oxidation of amines RNH_2 as well as

- (1) (a) Bryan, N. S.; Rassaf, T.; Maloney, R. E.; Rodriguez, C. M.; Saijo, F.; Rodriguez, J. R.; Feelisch, M. *Proc. Natl. Acad. Sci. U.S.A.* **2004**, *101*, 4308–4313. (b) Ischiropoulos, H.; Gow, A. *Toxicology* **2005**, *208*, 299–303. (c) Weichsel, A.; Maes, E. M.; Andersen, J. F.; Valenzuela, J. G.; Shokhireva, T. K.; Walker, F. A.; Montfort, W. R. *Proc. Natl. Acad. Sci. U.S.A.* **2005**, *102*, 594–599.
- (2) (a) Romeo, A. A.; Filosa, A.; Capobianco, J. A.; English, A. M. *J. Am. Chem. Soc.* **2001**, *123*, 1782–1783. (b) Romeo, A. A.; Capobianco, J. A.; English, A. M. *J. Am. Chem. Soc.* **2003**, *125*, 14370–14378. (c) Stubauer, G.; Giuffrè, A.; Sarti, P. *J. Biol. Chem.* **1999**, *274*, 28128–28133.
- (3) Stamlar, J. S.; Jia, L.; Eu, J. P.; McMahon, T. J.; Demchenko, I. T.; Bonaventura, J.; Gernert, K.; Piantadosi, C. A. *Science* **1997**, *276*, 2034–2037.
- (4) Ford, P. C.; Fernandez, B. O.; Lim, M. D. *Chem. Rev.* **2005**, *105*, 2439–2456.

- (5) Tsuge, K.; DeRosa, F.; Lim, M. D.; Ford, P. C. *J. Am. Chem. Soc.* **2004**, *126*, 6564–6565.

- (6) (a) Weiner, W. P.; White, M. A.; Bergman, R. G. *J. Am. Chem. Soc.* **1981**, *103*, 3612–3614. (b) Weiner, W. P.; Bergman, R. G. *J. Am. Chem. Soc.* **1983**, *105*, 3922–3929.

- (7) (a) Fletcher, S. R.; Skapski, A. C. *J. Organomet. Chem.* **1973**, *59*, 299–307. (b) Legzdins, P.; Rettig, S. J.; Sanchez, L. *Organometallics* **1988**, *7*, 2394–2403. (c) Fochi, G.; Floriani, C.; Chiesi-Villa, A.; Guastini, C. *J. Chem. Soc., Dalton Trans.* **1986**, 445–447.

- (8) Jones, C. J.; McCleverty, J. A.; Rothin, A. S. *J. Chem. Soc., Dalton Trans.* **1985**, 401–403.

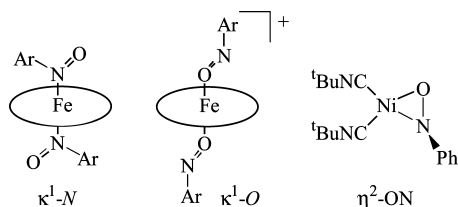


Figure 1. $[M](ONAr)$ bonding modes in representative mononuclear C -nitroso complexes.

the reduction of the corresponding nitro compounds RNO_2 .^{9,10} Motivated by the appreciably greater affinity of hemoglobin for nitrosobenzene ($PhNO$) over dioxygen (O_2),¹¹ a number of heme model complexes have been prepared.¹⁰ Typically, κ^1-N bonding of the nitrosoarene is observed in ferrous complexes,¹⁰ though κ^1-O bonding was observed in the ferric p -amino-substituted nitrosoarene adduct $[(TPP)Fe(ONAr)_2]^+$ ($TPP = meso$ -tetraphenylporphyrinato; Figure 1).¹² In the presence of both NADH and Cu(II) ions, nitrosobenzene elicits oxidative DNA damage through the intermediacy of the phenylhydronitroxide radical $PhNHO\cdot$.¹³ This nitroxide has also been identified as a metabolic product of $PhNO$ ¹⁴ (as well as $PhNH_2$, $PhNHOH$, and $PhNO_2$)¹⁵ that also participates in the oxidation of thiol residues within red blood cells.¹⁵

Additionally, organonitroso compounds $ArNO$ serve as precursors for copper-catalyzed $C-N$ bond-forming reactions^{16,17} as well as nickel-catalyzed nitrene-group transfer reactions.¹⁸ Srivastava showed that allylic $C-H$ bonds undergo amination in moderate yield by $ArNO$ or $ArNHOH$ under catalysis by Cu^I .¹⁶ As a part of those mechanistic studies, the trigonal tris(nitrosoarene)copper(I) adduct $[Cu(\kappa^1-N(O)Ar')_3]^+$ ($Ar' = p$ - $NEt_2C_6H_4$) was structurally characterized.¹⁶ Catalyzed by $Ni(CN^tBu)_4$, nitrene-group transfer reactions from $PhNO$ take place with CN^tBu , leading to tBuNCO and $PhN=C=N^tBu$ among other products.¹⁸ $Ni(\eta^2-ONPh)(CN^tBu)_2$, whose bonding mode (Figure 1) was assigned by IR spectroscopy ($\nu_{NO} = 1032\text{ cm}^{-1}$) was suggested as an active intermediate on the basis of its stoichiometric decomposition to $PhNHC(O)NH^tBu$ in the presence of trace water.¹⁸

A wide variety of $[M](RNO)$, $[M]_2(RNO)$, and $[M]_4(RNO)$ bonding modes in transition-metal C -nitroso complexes that involve varying degrees of $RN=O$ bond activation are known.¹⁰ The four-electron reductive cleavage of $ArN=O$ by the electron-rich, Co(I) β -diketiminato complex $[Me_2NN]Co(\eta^6\text{-toluene})$ to give $\{[Me_2NN]Co\}_2(\mu-O)(\mu-NAr)$ ($Ar = 3,5\text{-Me}_2C_6H_3$) repre-

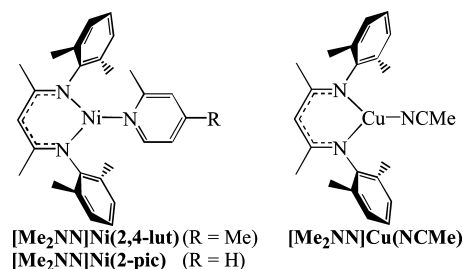
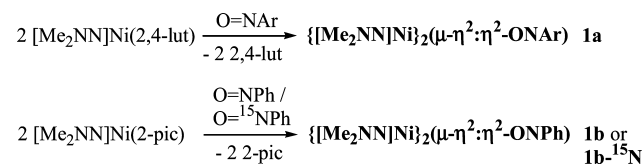


Figure 2. Structures of monovalent β -diketiminatonickel and -copper complexes employed in the synthesis of nitrosoarene adducts.

Scheme 1. Synthesis of Dinickel(I) Nitrosoarene Adducts 1



sents an extreme case of $RN=O$ bond activation.¹⁹ To systematically explore the effect of the metal ion on $ArN=O$ activation, we report herein the synthesis and structure of β -diketiminato $Ni(I)$ and $Cu(I)$ nitrosoarene adducts as well as their reactivity with NO to give divalent $NONOates$ ²⁰ $[Me_2NN]M(\eta^2-O_2N_2Ar)$.

Results and Discussion

Nickel Complexes. Addition of the nitrosoarene $ArN=O$ ($Ar = 3,5\text{-Me}_2C_6H_3$) to 2 equiv of $[Me_2NN]Ni(2,4\text{-lutidine})$ ²¹ (Figure 2) in ether allowed for the isolation of green crystals of $\{[Me_2NN]Ni\}_2(\mu\text{-}\eta^2\text{:}\eta^2\text{-ONAr})$ (**1a**) in 42% yield (Scheme 1). Single-crystal X-ray analysis revealed a symmetric, butterfly-shaped $[Ni]_2(ONAr)$ core with a pseudo mirror plane containing the $ArNO$ ligand linking the two Ni fragments (Figure 3). The $Ni-Ni$ separation is $3.171(2)\text{ \AA}$, and the $Ni-O$ bond distances are $1.881(3)$ and $1.932(3)\text{ \AA}$ with $Ni-N$ bond distances of $1.921(3)$ and $1.879(3)\text{ \AA}$. The $N-O$ distance of $1.440(4)\text{ \AA}$ is similar to that in $[(Cp^*Rh)_2(\mu\text{-Cl})(\mu\text{-}\eta^2\text{:}\eta^2\text{-ONPh})](BF_4)$ [$d_{N-O} = 1.422(4)\text{ \AA}$],²² indicating a significant reduction in $N-O$ bond order relative to that in free C -nitroso compounds, which possess $N-O$ distances in the range $1.13\text{--}1.29\text{ \AA}$.¹⁰

Because of the commercial availability of $Ph^{15}NH_2$, which allows for the ready preparation of $Ph^{15}NO$, characteristic ν_{NO} IR stretching frequencies were measured for the analogous nitrosobenzene adducts. The addition of $PhNO$ or $Ph^{15}NO$ to 2 equiv of $[Me_2NN]Ni(2\text{-picoline})$ {Figure 2; prepared analogously to $[Me_2NN]Ni(2,4\text{-lutidine})$ by substituting $NiCl_2(2\text{-pic})_2$ for $NiCl_2(2,4\text{-lut})_2$ in the synthesis procedure} allowed for the isolation of $\{[Me_2NN]Ni\}_2(\mu\text{-}\eta^2\text{:}\eta^2\text{-ONPh})$ (**1b** and **1b-¹⁵N**) (Scheme 1), which possess 1H NMR spectra closely related to that of **1a**. Coordination to two $[Me_2NN]Ni^I$ fragments markedly reduced the $PhNO$ ν_{NO} stretching frequency to 915 cm^{-1} (901 cm^{-1} for **1b-¹⁵N**) (Table 1) relative to that of free, monomeric $PhNO$ (1506 cm^{-1}).^{10,23}

Low-temperature 1H NMR spectra of **1a** at $-70\text{ }^\circ C$ in toluene- d_8 revealed four separate β -diketiminato $Ar-Me$ resonances,

- (9) Zuman, P.; Shah, B. *Chem. Rev.* **1994**, *94*, 1621–1641.
 (10) Lee, J.; Chen, L.; West, A. H.; Richter-Addo, G. B. *Chem. Rev.* **2002**, *102*, 1019–1066.
 (11) Eyer, P.; Ascherl, M. *Biol. Chem. Hoppe-Seyler* **1987**, *368*, 285–294.
 (12) Wang, L.-S.; Chen, L.; Khan, M. A.; Richter-Addo, G. B. *Chem. Commun.* **1996**, 323–324.
 (13) Ohkuma, Y.; Kawanishi, S. *Biochem. Biophys. Res. Commun.* **1999**, *257*, 555–560.
 (14) (a) Becker, A. R.; Sternson, L. A. *Bioorg. Chem.* **1980**, *9*, 305–312. (b) Takahashi, N.; Fischer, V.; Schreiber, J.; Mason, R. P. *Free Radical Res. Commun.* **1988**, *4*, 351–358. (c) Kiese, M.; Reinwein, D.; Waller, H. *Arch. Exp. Pathol. Pharmacol.* **1950**, *210*, 393–398.
 (15) Maples, K. R.; Eyer, P.; Mason, R. P. *Mol. Pharmacol.* **1990**, *37*, 311–318.
 (16) (a) Srivastava, R. S.; Khan, M. A.; Nicholas, K. M. *J. Am. Chem. Soc.* **2005**, *127*, 7278–7279. (b) Srivastava, R. S.; Tarver, N. R.; Nicholas, K. M. *J. Am. Chem. Soc.* **2007**, *129*, 15250–15258.
 (17) Yu, Y.; Srogl, J.; Liebeskind, L. S. *Org. Lett.* **2004**, *6*, 2631–2634.
 (18) Otsuka, S.; Aotani, Y.; Tatsuno, Y.; Yoshida, T. *Inorg. Chem.* **1976**, *15*, 656–660.

- (19) Dai, X.; Kapoor, P.; Warren, T. H. *J. Am. Chem. Soc.* **2004**, *126*, 4798–4799.
 (20) Hrabie, J. A.; Keefer, L. K. *Chem. Rev.* **2002**, *102*, 1135–1154.
 (21) Kogut, E.; Wiencko, H. L.; Zhang, L.; Cordeau, D. E.; Warren, T. H. *J. Am. Chem. Soc.* **2005**, *127*, 11248–11249.
 (22) Hoard, D. W.; Sharp, P. R. *Inorg. Chem.* **1993**, *32*, 612–620.
 (23) Calligaris, M.; Yoshida, T.; Otsuka, S. *Inorg. Chim. Acta* **1974**, *11*, L15–L16.

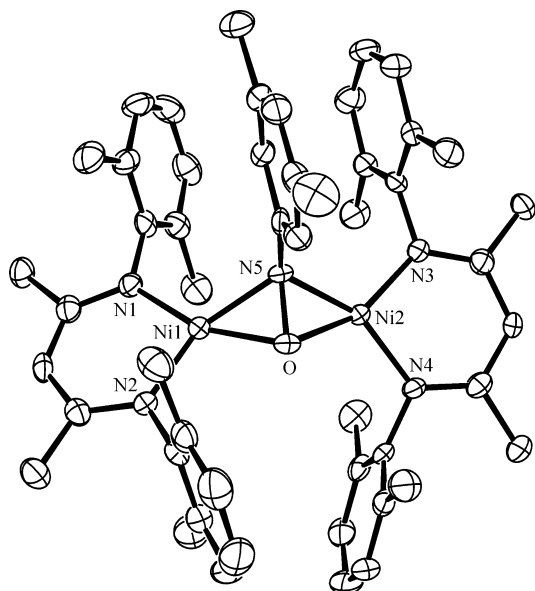


Figure 3. ORTEP diagram of the solid-state structure of $\{[\text{Me}_2\text{NN}]\text{Ni}\}_2(\mu\text{-}\eta^2\text{:}\eta^1\text{-ONAr})$ (**1a**) (with all H atoms omitted). Selected bond distances (Å) and angles (deg): N5–O, 1.440(4); Ni1–N5, 1.879(3); Ni2–N5, 1.921(3); Ni1–O, 1.932(3); Ni2–O, 1.881(3); Ni1–N1, 1.859(3); Ni1–N2, 1.868(3); Ni2–N3, 1.869(3); Ni2–N4, 1.868(3); N1–Ni1–N2, 94.88(14); N3–Ni2–N4, 96.36(15); N5–Ni1–O, 44.37(12); N5–Ni2–O, 44.48(12); Ni1–N5–Ni2, 113.09(16); Ni1–O–Ni2, 112.52(14); O–N5–C43, 112.8(3).

Table 1. ArN=O Distances and ν_{NO} Stretching Frequencies in Organonitroso Adducts **1–3**

compound	$d_{\text{N-O}}$ (Å)	$\nu^{14}\text{NO}/\nu^{15}\text{NO}$ (cm^{-1})
1a	1.440(4)	
1b	n/a	915/901
2a	1.375(6)	
2b	1.368(2)	1040/1029
3a	1.333(4)	
3b	1.336(6) ^a	1113/1093

^a Average of two independent distances.

consistent with the approximate C_s molecular symmetry observed in the solid state. Warming resulted in coalescence of two pairs of these Ar-Me resonances, suggesting rotation of one [Ni] fragment about the remaining [Ni](ONAr) unit in **1a** with an activation barrier (ΔG^\ddagger) of 10.2(3) kcal/mol at $-50(3)^\circ\text{C}$. While the diamagnetic ^1H NMR chemical shifts of **1a** were otherwise unremarkable, the backbone-CH and backbone-Me signals were mildly temperature-dependent in toluene- d_8 . Over the temperature range -70 to $+25^\circ\text{C}$, these two signals shifted upfield from 4.66 to 3.48 ppm and 1.01 to 0.49 ppm, respectively. These observations suggest contact shifts from a minute contribution of a higher spin state in solution.²⁴ DFT studies on **1a** (gas phase) identified an $S = 1$ excited state ~ 12 kcal/mol higher in electronic energy bearing metrical parameters similar to those of the $S = 0$ ground state [Figure S7 in the Supporting Information (SI)]. In the $S = 1$ state, there is significant unpaired electron density (spin- α) on the central C atom of the β -diketiminato ligand (Figure 4). Variable-temperature solid-state magnetic susceptibility measurements on **1a** gave a steadily increasing magnetic moment that reached $2.6\mu_{\text{B}}$ at 300 K, which is close to the spin-only value of $2.8\mu_{\text{B}}$ expected for an $S = 1$ system (Figure S10 in the SI).

(24) Melzer, M. M.; Jarchow-Choy, S.; Kogut, E.; Warren, T. H. *Inorg. Chem.* **2008**, *47*, 10187–10189.

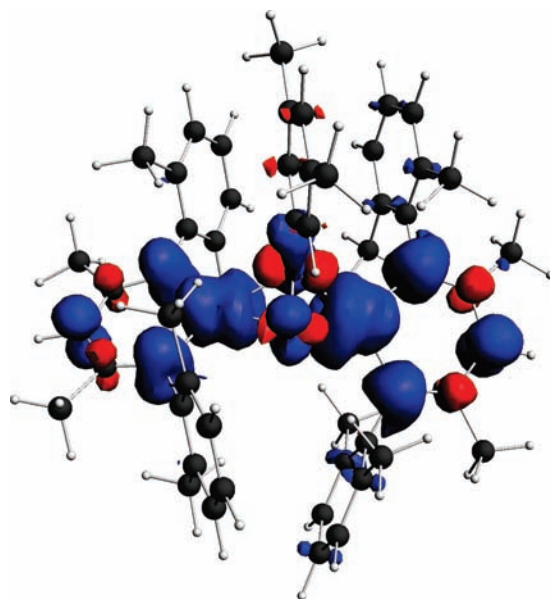
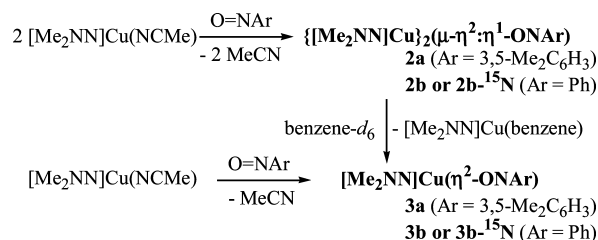


Figure 4. Spin density plot for **1a** ($S = 1$). Blue indicates excess spin- α ; red indicates excess spin- β (isospin value = 0.001).

Scheme 2. Synthesis of Cu(I) Nitrosoarene Adducts **2** and **3**



Copper Complexes. Reaction of the Cu(I) β -diketiminato complex $[\text{Me}_2\text{NN}]\text{Cu}(\text{NCMe})$ ²⁵ (Figure 2) with 0.5 equiv of ArNO resulted in the formation of a very dark solution from which crystals of $\{[\text{Me}_2\text{NN}]\text{Cu}\}_2(\mu\text{-}\eta^2\text{:}\eta^1\text{-ONAr})$ (**2a**) could be isolated in modest yield from ether (Scheme 2). Unlike the one in **1a**, the nitrosoarene ligand in **2a** is η^2 -bound to one Cu center with Cu1–O and Cu1–N5 distances of 1.843(4) and 2.040(5) Å and bound only through the N atom to the other Cu center with a Cu2–N5 distance of 1.879(5) Å (Figure 5). The N–O bond is less activated than in **1a**, with a N–O distance of 1.375(6) Å. The related complex $\{[\text{Me}_2\text{NN}]\text{Cu}\}_2(\mu\text{-}\eta^2\text{:}\eta^1\text{-ONPh})$ (**2b**) possesses similar metrical parameters (N5–O, 1.368(2) Å; Cu1–O, 1.840(2) Å; Cu1–N5, 2.013(2) Å; Cu2–N5, 1.900(2) Å; Figure S19 in the SI) and shows a ν_{NO} stretch at 1040 cm^{-1} (1029 cm^{-1} for **2b-}^{15}\text{N}) (Table 1).**

This asymmetry suggested that one $[\text{Me}_2\text{NN}]\text{Cu}$ fragment of **2a** may be labile in solution. Dissolution of crystals of **2a** in benzene- d_6 resulted in the quantitative formation of mononuclear $[\text{Me}_2\text{NN}]\text{Cu}(\eta^2\text{-ONAr})$ (**3a**) with formation of the solvento species $[\text{Me}_2\text{NN}]\text{Cu}(\text{benzene})$ ²⁶ (Scheme 2).

Reaction of $[\text{Me}_2\text{NN}]\text{Cu}(\text{NCMe})$ with 1 equiv of ArNO allowed for the isolation of mononuclear **3a** (Scheme 2) possessing nearly symmetric η^2 -NO bonding with Cu–N3 and

(25) Spencer, D. J. E.; Reynolds, A. M.; Holland, P. L.; Jazdzewski, B. A.; Duboc-Toia, C.; Le Pape, L.; Yokota, S.; Tachi, Y.; Itoh, S.; Tolman, W. B. *Inorg. Chem.* **2002**, *41*, 6307–6321.

(26) (a) Dai, X.; Warren, T. H. *J. Am. Chem. Soc.* **2004**, *126*, 10085–10094. (b) Amisial, L. D.; Dai, X.; Kinney, R. A.; Krishnaswamy, A.; Warren, T. H. *Inorg. Chem.* **2004**, *43*, 6537–6539.

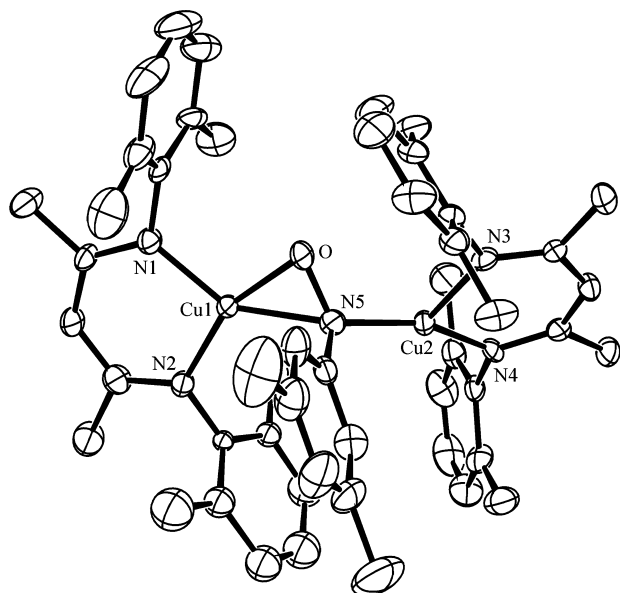


Figure 5. ORTEP diagram of $\{[\text{Me}_2\text{NN}]\text{Cu}\}_2(\mu\text{-}\eta^2\text{:}\eta^1\text{-ONAr})$ (**2a**) $\cdot \frac{1}{2}\text{Et}_2\text{O}$ (with all H atoms and ether of solvation omitted; the major occupancy (55%) of the disordered β -diketiminato *N*-aryl ring at N2 is shown). Selected bond distances (Å) and angles (deg): N5–O, 1.375(6); Cu1–N5, 2.040(5); Cu2–N5, 1.879(5); Cu1–O, 1.843(4); Cu2···O, 2.786; Cu1–N1, 1.891(5); Cu1–N2, 1.891(5); Cu2–N3, 1.984(5); Cu2–N4, 1.907(5); N1–Cu1–N2, 99.9(2); N3–Cu2–N4, 100.16(19); N5–Cu1–O, 41.10(18); Cu1–N5–Cu2, 140.2(3); O–N5–C43, 110.3(5).

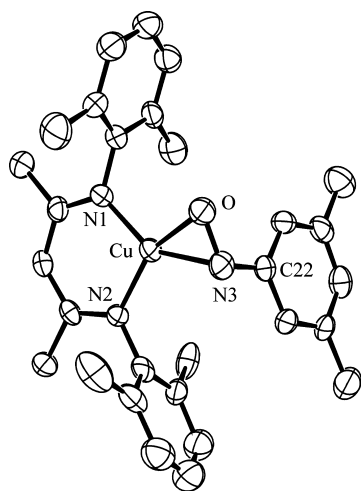
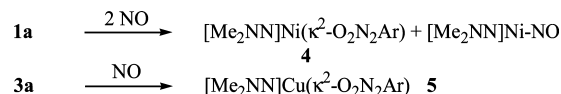


Figure 6. ORTEP diagram of the solid-state structure of $[\text{Me}_2\text{NN}]\text{Cu}(\eta^2\text{-ONAr})$ (**3a**) (with all H atoms omitted). Selected bond distances (Å) and angles (deg): N3–O, 1.333(4); Cu–N3, 1.936(4); Cu–O, 1.851(3); Cu–N1, 1.886(3); Cu–N2, 1.884(3); N3–C22, 1.441(6); N3–Cu–O, 41.14(14); N1–Cu–N2, 99.96(15); N1–Cu–O, 106.69(14); N2–Cu–N3, 112.92(15).

Cu–O bond distances of 1.936(4) and 1.851(3) Å, respectively (Figure 6). $[\text{Me}_2\text{NN}]\text{Cu}(\eta^2\text{-ONAr})$ (**3a**) possesses the least-activated ArN=O bond, with a N–O bond distance of 1.333(4) Å, which is shorter than the range of 1.386(3)–1.432(6) Å established for other mononuclear $\eta^2\text{-ONR}$ compounds.¹⁰ The X-ray structure of the corresponding nitrosobenzene adduct $[\text{Me}_2\text{NN}]\text{Cu}(\eta^2\text{-ONPh})$ (**3b**) possesses two independent molecules of **3b** with similar metrical parameters (N3–O, 1.338(5) and 1.334(5) Å; Cu–N3, 1.932(4) and 1.935(3) Å; Cu–O, 1.853(3) and 1.855(3) Å; Figures S22 and S23 in the SI). Consistent with the lowest degree of N–O bond activation inferred by N–O bond lengths, this mononuclear nitrosobenzene

Scheme 3. Reactivity of Nitrosoarene Adducts with Nitric Oxide



adduct exhibits the highest ν_{NO} at 1113 cm^{-1} (1093 cm^{-1} for **3b**-¹⁵N) among **1b**, **2b**, and **3b** (Table 1).

Despite the larger size of N compared with O, the N–O distance in **3a** is significantly shorter than the O–O distances of 1.392(12) and 1.392(3) Å found in Tolman's side-on copper dioxygen complexes $[\text{Cu}](\eta^2\text{-O}_2)$ supported by β -diketiminato and anilidoimine ligands.²⁷ Both of these considerations suggest modest backbonding from the $[\text{Me}_2\text{NN}]\text{Cu}$ fragment to the nitrosoarene. Indeed, the $\eta^2\text{-ArN=O}$ binding mode in **3** is reminiscent of η^2 -coordination of an alkene to Cu(I).²⁸ Variable-temperature NMR spectra of **3b** revealed a modest activation barrier for rotation about the Cu–ArNO moiety $\{\Delta G^\ddagger = 11.4(2)$ kcal/mol at $-44(2)$ °C, which is similar to the value of 10.7(3) kcal/mol observed for $[\text{Me}_2\text{NN}]\text{Cu}(\eta^2\text{-styrene})$ ²⁹ }.

Arylnitroso coordination to the $[\text{Me}_2\text{NN}]\text{Cu}^{\text{I}}$ fragment, however, has a significant effect on the oxidation potential of the copper(I) center. Cyclic voltammetry of **3a** in MeCN revealed an essentially irreversible oxidation at ca. +1.1 V versus NHE referenced against an internal ferrocene standard (+0.48 V vs ferrocene/ferrocenium) (Figure S11 in the SI). This may be compared with the value of +0.45 V versus NHE reported for the simple $[\text{Me}_2\text{NN}]\text{Cu}(\text{NCMe})$ adduct.²⁵

Reactions with Nitric Oxide. The Ni(I) and Cu(I) nitrosoarene adducts **1a** and **3a** react with NO(g) under anaerobic conditions (Scheme 3). Addition of 2.1 equiv of NO to a benzene-*d*₆ solution of **1a** resulted in the quantitative formation of the diamagnetic $[\text{Me}_2\text{NN}]\text{Ni}(\kappa^2\text{-O}_2\text{N}_2\text{Ar})$ ³⁰ (**4**) and $[\text{Me}_2\text{NN}]\text{Ni}(\text{NO})$,³⁰ which were identified by ¹H NMR spectroscopy. It should be noted that **4** forms quickly upon addition of ArNO to the nickel nitrosyl $[\text{Me}_2\text{NN}]\text{Ni}(\text{NO})$.³⁰ Perhaps more surprising was the uptake of NO by $[\text{Me}_2\text{NN}]\text{Cu}(\eta^2\text{-ONAr})$ (**3a**) to give red crystals of $[\text{Me}_2\text{NN}]\text{Cu}(\kappa^2\text{-O}_2\text{N}_2\text{Ar})$ (**5**) in 80% yield when **3a** was exposed to a slight excess of NO (2 equiv). The X-ray structure of **5** (Figure 7) shows square-planar coordination at Cu, as found in the structures of $\text{Cu}(\kappa^2\text{-O}_2\text{N}_2\text{R})_2$ (R = Ph,³¹ Cy³²). The EPR spectrum of **5** in toluene at room temperature is consistent with a Cu(II) ion in a square-planar environment with two N donors ($g_{\text{iso}} = 2.10$, $A_{\text{Cu}} = 79$ G, $A_{\text{N}} = 13$ G).

In contrast to typical reductive nitrosylation reactions, in which the metal center is reduced with concomitant oxidation of the organic fragment,⁴ the reaction between $[\text{Me}_2\text{NN}]\text{Cu}(\eta^2\text{-ONAr})$ and NO may formally proceed through oxidation of the copper complex to $\{[\text{Me}_2\text{NN}]\text{Cu}(\eta^2\text{-ONAr})\}^+$ and reduction of NO to NO[−]. However, the high oxidation potential for $[\text{Me}_2\text{NN}]\text{Cu}(\eta^2\text{-ONAr})$ ($E_{1/2} \approx +1.1$ V vs NHE) as well as the high reduction

(27) (a) Aboeella, N. W.; Lewis, E. A.; Reynolds, A. M.; Brennessel, W. W.; Cramer, C. J.; Tolman, W. B. *J. Am. Chem. Soc.* **2002**, *124*, 10660–10661. (b) Aboeella, N. W.; Kryatov, S. V.; Gherman, B. F.; Brennessel, W. W.; Young, V. G., Jr.; Sarangi, R.; Rybak-Akimova, E. V.; Hodgson, K. O.; Hedman, B.; Solomon, E. I.; Cramer, C. J.; Tolman, W. B. *J. Am. Chem. Soc.* **2004**, *126*, 16896–16911. (c) Reynolds, A. M.; Gherman, B. F.; Cramer, C. J.; Tolman, W. B. *Inorg. Chem.* **2005**, *44*, 6989–6997.

(28) Rasika Dias, H. V.; Wu, J. *Eur. J. Inorg. Chem.* **2008**, 509–522.

(29) Dai, X.; Warren, T. H. *Chem. Commun.* **2001**, 1998–1999.

(30) Puiui, S. C.; Warren, T. H. *Organometallics* **2003**, *22*, 3974–3976.

(31) Shkol'nikov, L. M.; Shugam, E. A. *Zh. Strukt. Khim.* **1963**, *4*, 380–386.

(32) Klebe, G.; Hädicke, E.; Boehm, K. H.; Reuther, W.; Hickmann, E. Z. *Kristallogr.* **1996**, *211*, 798–803.

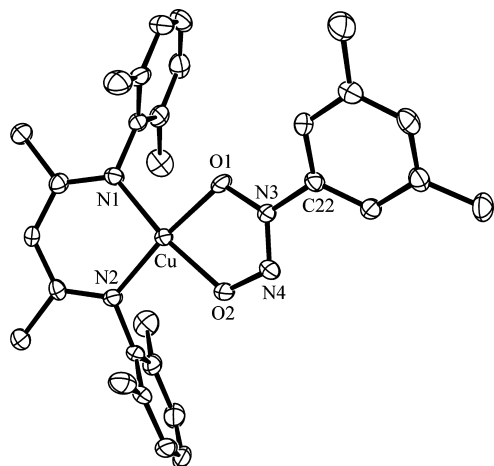


Figure 7. ORTEP diagram of the solid-state structure of $[\text{Me}_2\text{NN}]\text{Cu}(\kappa^2\text{-O}_2\text{N}_2\text{Ar})$ (**5**) (with all H atoms omitted). Selected bond distances (Å) and angles (deg): Cu–O1, 1.957(2); Cu–O2, 1.949(2); Cu–N1, 1.931(3); Cu–N2, 1.929(3); O1–N3, 1.323(3); O2–N4, 1.306(3); N3–N4, 1.282(4); N1–Cu–N2, 95.59(12); O1–Cu–O2, 79.23(10); N1–Cu–O1, 93.19(11); N2–Cu–O2, 92.33(10).

potential for NO to NO^- [estimated at -0.8 V vs NHE for 1 M $\text{NO}(\text{aq})$ ³³] strongly suggest inner-sphere attack of NO on $[\text{Me}_2\text{NN}]\text{Cu}(\eta^2\text{-ONAr})$.

Conclusions

The two-coordinate, monovalent fragments $[\text{Me}_2\text{NN}]\text{M}$ ($\text{M} = \text{Ni}, \text{Cu}$) favor π interactions with the $\text{ArN}=\text{O}$ bond of *C*-nitroso compounds, thereby providing what are to the best of our knowledge the first X-ray structures of Ni and Cu *C*-nitroso adducts in which the NO functionality is not $\kappa^1\text{-N}$ -bound.^{10,16} We note that a recent theoretical study suggested that $\eta^2\text{-ONPh}$ coordination in copper(I) β -diketimines may be slightly favored over $\kappa^1\text{-N}$ bonding³⁴ and that IR data suggest side-on nitrosobenzene coordination in the zero-valent complex $\text{Ni}(\text{ONPh})(\text{CN}^t\text{Bu})_2$ (Figure 1).¹⁸

The dinuclear complexes $\{[\text{Me}_2\text{NN}]\text{Ni}\}_2(\mu\text{-}\eta^2\text{:}\eta^2\text{-ONAr})$ (**1**) are conceptually related to the dinuclear toluene adduct $\{[\text{Nacnac}]\text{Ni}\}_2(\mu\text{-}\eta^3\text{:}\eta^3\text{-toluene})$ of a related $[\beta\text{-diketiminato}]\text{Ni}^{\text{I}}$ fragment that possesses *o*-ⁱPr *N*-aryl substituents.³⁵ The monovalent, mononuclear $[\text{Me}_2\text{NN}]\text{Ni}(\eta^2\text{-ONAr})$ fragment likely possesses a significant amount of unpaired electron density on the $\eta^2\text{-ON}$ moiety, as found on the $\eta^2\text{-O}_2$ ligand in the square-planar superoxide complex $[\text{Nacnac}]\text{Ni}(\eta^2\text{-O}_2)$.³⁶ Thus, the mononuclear species $[\text{Me}_2\text{NN}]\text{Ni}(\eta^2\text{-ONAr})$ would be a ready target for the less sterically hindered $[\text{Me}_2\text{NN}]\text{Ni}$ metalloradical to give **1**. Perhaps more unusual is the unsymmetrical metal–organonitroso interaction in $\{[\text{Me}_2\text{NN}]\text{Cu}\}_2(\mu\text{-}\eta^2\text{:}\eta^1\text{-ONAr})$ (**2**), in which the $\kappa^1\text{-N}$ interaction is readily displaced by benzene to give $[\text{Me}_2\text{NN}]\text{Cu}(\eta^2\text{-ONAr})$ (**3**) and $[\text{Me}_2\text{NN}]\text{Cu}(\text{benzene})$.

The *C*-nitroso adducts reported herein are capable of incorporating 1 equiv of NO into the coordinated ONAr ligand to

form diazeniumdiolates $[\text{M}](\kappa^2\text{-O}_2\text{N}_2\text{Ar})$, which represents oxidative nitrosylation of the formally monovalent $[\text{Me}_2\text{NN}]\text{Cu}(\eta^2\text{-ONAr})$. This serves as a well-defined example that illustrates the possibility of oxidizing a metal center via functionalization of a bound ligand with NO.

The $\eta^2\text{-ONAr}$ binding modes and reactivity observed in the organonitroso complexes $\{[\text{Me}_2\text{NN}]\text{Ni}\}_2(\mu\text{-}\eta^2\text{:}\eta^2\text{-ONAr})$ (**1**), $\{[\text{Me}_2\text{NN}]\text{Cu}\}_2(\mu\text{-}\eta^2\text{:}\eta^1\text{-ONAr})$ (**2**), and $[\text{Me}_2\text{NN}]\text{Cu}(\eta^2\text{-ONAr})$ (**3**) may foreshadow possibilities in related “parent” HNO ³⁷ adducts. For instance, aromatic nitroso compounds ArNO have been considered as *N*-substituted nitroxyls,³⁸ and PhNO rapidly reacts with HNO (but not NO) to give Cupferron $[\text{HON}(\text{Ph})\text{N}=\text{O}]$,³⁹ the conjugate acid of the diazeniumdiolate anion $[\text{O}_2\text{N}_2\text{Ph}]^-$. Nonetheless, one must bear in mind HNO ’s distinct acid/base behavior ($\text{p}K_{\text{a}} = 11.4$),^{33,40} facile oxidation ($\text{HNO}/\text{NO}, \text{H}^+ = +0.5$ to $+0.6$ V at pH 7),^{33,40} H atom transfer ($\text{H}-\text{NO}$ bond dissociation energy ≈ 50 kcal/mol),⁴¹ and rapid, irreversible dimerization ($k = 8 \times 10^6 \text{ M}^{-1} \text{ s}^{-1}$ in aqueous solution)⁴⁰ chemistry. To date, synthetic examples of $[\text{M}](\text{HNO})$ complexes exhibit $\kappa^1\text{-N}$ bonding and have been limited to low-spin, d^6 octahedral complexes.⁴²

Experimental Section

General Considerations. All of the experiments were carried out under a dry nitrogen atmosphere using an MBraun glovebox and/or standard Schlenk techniques. Activation of 4 Å molecular sieves was carried out in vacuo at 180 °C for 24 h. Diethyl ether and tetrahydrofuran (THF) were first sparged with nitrogen and then dried by passage through activated alumina columns.⁴³ Pentane was first washed with concentrated $\text{HNO}_3/\text{H}_2\text{SO}_4$ to remove olefins, stored over CaCl_2 , and then distilled from sodium/benzophenone before use. All of the deuterated solvents were sparged with nitrogen, dried over activated 4 Å molecular sieves, and stored under nitrogen. ¹H and ¹³C NMR spectra were recorded on a Varian 300 or 400 MHz spectrometer (300 or 400 and 75.4 or 100.4 MHz, respectively). All of the NMR spectra were recorded at room temperature (RT) unless otherwise noted and were indirectly referenced to tetramethylsilane using residual solvent signals as internal standards. X-band EPR spectra were recorded in toluene at RT in a quartz tube using a Bruker EMX-A spectrometer control system equipped with a Bruker B-E2549 10 in. magnet and a built-in microwave frequency meter. Elemental analyses were performed on a PerkinElmer PE2400 microanalyzer in our laboratories.

Cyclic voltammetry on **3a** (Figure S11 in the SI) was performed in 0.1 M $[\text{NBu}_4]\text{BF}_4/\text{MeCN}$ using a Schlenk flask as the standard cell. The auxiliary and working electrodes were 500 and 250 μm platinum wires, respectively. A nonaqueous reference electrode was

- (33) Bartberger, M. D.; Liu, W.; Ford, E.; Miranda, K. M.; Switzer, C.; Fukuto, J. M.; Farmer, P. J.; Wink, D. A.; Houk, K. N. *Proc. Natl. Acad. Sci. U.S.A.* **2002**, *99*, 10958–10963.
 (34) Kazi, A. B.; Cundari, T. R.; Baba, E.; DeYonker, N. J.; Dinescu, A.; Spaine, L. *Organometallics* **2007**, *26*, 910–914.
 (35) Bai, G.; Wei, P.; Stephan, D. W. *Organometallics* **2005**, *24*, 5901–5908.
 (36) Yao, S.; Bill, E.; Milsmann, C.; Wieghardt, K.; Driess, M. *Angew. Chem., Int. Ed.* **2008**, *47*, 7110–7113.

- (37) (a) Fukuto, J. M.; Bartberger, M. D.; Dutton, A. S.; Paolucci, N.; Wink, D. A.; Houk, K. N. *Chem. Res. Toxicol.* **2005**, *18*, 790–801. (b) Miranda, K. M.; Ridnour, L. A.; Espey, M. G.; Citrin, D.; Thomas, D. D.; Mancardi, D.; Donzelli, S.; Wink, D. A.; Katori, T.; Tocchetti, C. G.; Ferlito, M.; Paolucci, N.; Fukuto, J. M. *Prog. Inorg. Chem.* **2005**, *54*, 349–384. (c) Paolucci, N.; Jackson, M. I.; Lopez, B. E.; Miranda, K.; Tocchetti, C. G.; Wink, D. A.; Hobbs, A. J.; Fukuto, J. M. *Pharmacol. Ther.* **2007**, *113*, 442–458. (d) Irvine, H. C.; Ritchie, R. H.; Favaloro, J. L.; Andrews, K. L.; Widdop, R. E.; Kemp-Harper, B. K. *Trends Pharmacol. Sci.* **2008**, *29*, 601–608.
 (38) Nagasawa, H. T.; Yost, Y.; Eberling, J. A.; Shirota, F. N.; DeMaster, E. G. *Biochem. Pharmacol.* **1993**, *45*, 2129–2134.
 (39) Shoeman, D. W.; Nagasawa, H. T. *Nitric Oxide* **1998**, *2*, 66–72.
 (40) Shafirovich, V.; Lyman, S. V. *Proc. Natl. Acad. Sci. U.S.A.* **2002**, *99*, 7340–7345.
 (41) (a) Bartberger, M. D.; Fukuto, J. M.; Houk, K. N. *Proc. Natl. Acad. Sci. U.S.A.* **2001**, *98*, 2194–2198. (b) Gomes, J. R. B.; Ribeiro da Silva, M. D. M. C.; Ribeiro da Silva, M. A. V. *J. Phys. Chem. A* **2004**, *108*, 2119–2130.
 (42) Farmer, P. J.; Sulc, F. *J. Inorg. Biochem.* **2005**, *99*, 166–184.
 (43) Pangborn, A. B.; Giardello, M. A.; Grubbs, R. H.; Rosen, R. K.; Timmers, F. J. *Organometallics* **1996**, *15*, 1518–1520.

used with 0.01 M AgNO₃ in 0.1 M [NBu₄]BF₄/MeCN as the electrolyte solution. Potential was applied using an IBM model 225 Radiometer Voltalab 10 potentiostat; current was applied and monitored throughout cycling between -400 and +1000 mV relative to the Ag reference electrode.

The nitrosoarene ArN=O (Ar = 3,5-Me₂C₆H₃),¹⁹ [Me₂NN]Ni(2,4-lutidine),²¹ [Me₂NN]Cu(MeCN),²⁵ and Ti[Me₂NN]²⁹ were synthesized according to literature procedures. ¹⁵N-labeled aniline (Ph¹⁵NH₂) was purchased from Cambridge Isotope Laboratories.

Preparation of Compounds. [¹⁵N]Nitrosobenzene (Ph¹⁵NO). Ph¹⁵NO was prepared by a procedure analogous to that used for 3,5-dimethylnitrosobenzene.¹⁹ To a solution of ¹⁵N-labeled aniline (1.00 g, 10.8 mmol) in a 1:1 pentane/dichloromethane mixture (100 mL) was added Na₂WO₄·2H₂O (0.171 g, 0.52 mmol), tetrabutylammonium chloride (0.043 g, 0.15 mmol), and 30% aqueous hydrogen peroxide (5 mL). The mixture was vigorously stirred for 18 h at RT. The organic layer was separated, washed with 0.01 M HCl (50 mL) followed by water (50 mL), and then dried over anhydrous MgSO₄. The organic layer was concentrated to dryness, and the resulting oil was crystallized using 1:1 pentane/dichloromethane to afford 0.70 g (60% yield) of the product as brown crystals. ¹H NMR (C₆D₆, RT): δ 7.596 (m, 2H, Ar-H), 6.976 (m, 3H, Ar-H). ¹³C{¹H} NMR (C₆D₆): δ 166.13, 165.97, 135.06, 129.22, 120.69, 120.63. IR: ν¹⁵_{NO} = 1353 cm⁻¹ (from PhNO dimer).¹⁰

{[Me₂NN]Ni}₂(μ-η²:η²-ONAr) (1a). A solution of 3,5-dimethylnitrosobenzene (0.015 g, 0.11 mmol) in ether (3 mL) was slowly added with stirring to a solution of [Me₂NN]Ni(2,4-lutidine) (0.108 g, 0.23 mmol) in ether (10 mL). The solution was stirred for 1 h and then filtered through Celite, and the filtrate was concentrated and cooled to -35 °C. The green crystals that had formed were separated from the solution, washed with cold pentane, and dried in vacuo to afford 0.042 g (42% yield) of the product. Recrystallization from pentane afforded green crystals suitable for X-ray diffraction. ¹H NMR (C₆D₆, RT): δ 7.095 (d, 4H, *m*-Ar-H), 6.887 (d, 4H, *m*-Ar-H), 6.509 (s, 1H, *p*-ArNO-H), 6.456 (t, 6H, *p*-Ar-H + *o*-ArNO-H), 3.476 (s, 2H, backbone-CH), 3.029 (s, 12H, *o*-Ar-Me), 2.279 (s, 12H, *o*-Ar-Me), 2.192 (s, 6H, ArNO-Me), 0.485 (s, 12H, backbone-Me). ¹³C{¹H} NMR (C₆D₆): δ 162.82, 160.46, 159.82, 136.42, 132.00, 122.02, 102.48, 98.21, 24.00, 21.08, 16.86 (two signals obscured). UV-vis (Et₂O): λ_{max} = 615 nm (ε = 1100 M⁻¹ cm⁻¹). Anal. Calcd for C₅₀H₅₉O₁N₅Ni₂: C, 69.55; H, 6.88; N, 8.11. Found: C, 69.60; H, 6.97; N, 8.34.

¹H NMR (-70 °C, toluene-*d*₈): δ 7.514 (s, 1H, *p*-ArNO), 6.87–6.56 (br, 14H, ArH), 4.662 (s, 2H, backbone-CH), 2.980 (s, 6H, *o*-Ar-Me), 2.617 (s, 6H, *o*-Ar-Me), 2.282 (s, 6H, *o*-Ar-Me), 1.989 (s, 6H, ArNO-Me), 1.549 (s, 6H, *o*-Ar-Me), 1.006 (s, 12H, backbone-Me). Coalescence of the two *o*-Ar-Me peaks at 2.980 and 2.617 ppm (300 MHz) gave Δ*G*[‡] = 10.3(2) kcal/mol at -55(3) °C; coalescence of the two *o*-Ar-Me peaks at 2.282 and 1.549 ppm (300 MHz) gave Δ*G*[‡] = 10.2(2) kcal/mol at -50(3) °C.

[Me₂NN]Ni(2-picoline). A solution of Ni(2-picoline)₂Cl₂ (2.00 g, 6.33 mmol) (prepared analogously to Ni(2,4-lutidine)₂Cl₂⁴⁴) in 30 mL of THF was added to a solution of [Me₂NN]Ti (3.22 g, 6.33 mmol) in 50 mL of THF. The reaction mixture was allowed to stir for 1 h and then was passed through Celite. Na/Hg [38.7 g, 0.5% (w/w) Na] was added to the reaction mixture, and a color change to red was observed after vigorous shaking. The solution was stirred for an additional 3 h, after which it was decanted off and passed through Celite. All of the volatiles were removed in vacuo. The remaining solid was recrystallized from Et₂O at -35 °C to afford 1.40 g (49% yield) of red crystals, which were dried in vacuo. UV-vis (Et₂O): λ_{max} = 522 nm (ε = 1000 M⁻¹ cm⁻¹). EPR (X-band, toluene glass, 90 K, with a small amount of added 2-picoline): *g*₁ = 2.41, *g*₂ = 2.12, *g*₃ = 2.06. Anal. Calcd for C₂₇H₃₂N₃Ni: C, 70.92; H, 7.05; N, 9.19. Found: C, 70.73; H, 7.46; N, 9.20.

{[Me₂NN]Ni}₂(μ-η²:η²-ONPh) (1b). A solution of nitrosobenzene (0.024 g, 0.22 mmol) in toluene (3 mL) was slowly added with stirring to a solution of [Me₂NN]Ni(2-picoline) (0.203 g, 0.44 mmol) in ether (10 mL). The solution was stirred for 1 h, concentrated to dryness, taken up in ether (10 mL), and filtered through Celite. The filtrate was concentrated and cooled to -35 °C. The green crystals were isolated to afford 0.109 g (30% yield) of product. ¹H NMR (C₆D₆, RT): δ 7.083 (d, 5H, Ar-H), 6.870 (m, 7H, Ar-H), 6.452 (t, 5H, Ar-H), 5.210 (br, 1H, *p*-PhNO-H), 3.495 (2H, backbone-CH), 3.010 (s, 12H, *o*-Ar-Me), 2.264 (s, 12H, *o*-Ar-Me), 0.487 (s, 12H, backbone-Me). ¹³C{¹H} NMR (C₆D₆): δ 164.39, 152.37, 151.06, 150.38, 147.26, 137.68, 137.40, 136.23, 126.85, 126.57, 125.02, 122.73, 106.30, 65.89, 27.37, 26.69, 19.18, 18.22, 17.32, 15.58. IR: ν_{NO} = 915 cm⁻¹ (901 cm⁻¹ for **1b**-¹⁵N). UV-vis (Et₂O): λ_{max} = 583 nm (ε = 2000 M⁻¹ cm⁻¹). The RT ¹H NMR spectra of **1a** and **1b** were nearly superimposable except for the ONAr and ONPh signals (Figures S1 and S2).

{[Me₂NN]Cu}₂(μ-η²:η¹-ONAr) (2a). A solution of ArNO (0.046 g, 0.34 mmol) in ether (5 mL) was slowly added with stirring to a solution of [Me₂NN]Cu(MeCN) (0.290 g, 0.68 mmol) in ether (15 mL). The solution turned dark immediately. The solution was stirred for 30 min and then filtered through Celite, after which the filtrate was concentrated and cooled to -35 °C. Black crystals were separated from the solution, washed with cold pentane, and dried in vacuo to afford 0.094 g (30% yield) of the product. This dinuclear species dissociates in benzene-*d*₆ to give [Me₂NN]Cu(η²-ONAr) (**3**) and [Me₂NN]Cu(benzene).²⁶ ¹H NMR (C₆D₆): δ 7.11–6.96 (m, 12H, Ar-H), 6.751 (s, 1H, *p*-ArNO-H (**3**)), 6.596 (s, 2H, *o*-ArNO-H (**3**)), 4.771 (s, 2H, backbone-CH (both **3** and [Cu](benzene)), 2.174 (br, 12H, *o*-Ar-Me (**3**)), 2.046 (s, 6H, *m*-ArNO-Me (**3**)), 2.012 (s, 6H, *o*-Ar-Me ([Cu](benzene)), 1.629 (s, 6H, backbone-Me ([Cu](benzene)), 1.445 (s, 6H, backbone-Me (**3**)). ¹³C{¹H} NMR (C₆D₆): δ 163.24, 162.43, 160.88, 150.56, 147.90, 138.61, 132.08, 130.61, 129.77, 128.44, 125.00, 123.13, 118.28, 95.81, 93.07, 23.13, 22.87, 21.01, 18.83, 18.50. UV-vis (Et₂O): λ_{max} = 582 nm (ε = 1400 M⁻¹ cm⁻¹), 791 nm (ε = 2000 M⁻¹ cm⁻¹). Anal. Calcd for C₅₀H₅₉O₁N₅Cu₂: C, 68.78; H, 6.81; N, 8.02. Found: C, 68.50; H, 6.82; N, 7.90.

The UV-vis molar absorptivities are approximate: the higher-energy band at λ = 582 nm corresponds to [Me₂NN]Cu(η²-ONAr) (**3b**) from dissociation of a [Me₂NN]Cu fragment in dilute solution.

{[Me₂NN]Cu}₂(μ-η²:η¹-ONPh) (2b). A solution of PhNO (0.036 g, 0.34 mmol) in ether (5 mL) was slowly added with stirring to a solution of [Me₂NN]Cu(MeCN) (0.279 g, 0.68 mmol) in ether (10 mL). The solution turned dark immediately. The solution was stirred for 1 h and then filtered through Celite, after which the filtrate was concentrated to dryness. Crystallization from pentane at -35 °C afforded 0.199 g (67% yield) of dark crystals of the product. This dinuclear species dissociates in benzene-*d*₆ to give [Me₂NN]Cu(η²-ONPh) and [Me₂NN]Cu(benzene).⁷ ¹H NMR (C₆D₆, RT): δ 7.026 (m, 15H, Ar-H), 6.840 (d, 2H, Ar-H), 6.755 (t, 3H, Ar-H), 4.772 (s, 1H, backbone-CH for [Me₂NN]Cu(benzene)), 4.762 (s, 1H, backbone-CH for [Me₂NN]Cu(η²-ONPh)), 2.127 (br, 12H, *o*-Ar-Me for [Me₂NN]Cu(η²-ONPh)), 2.012 (s, 12H, Me), 1.630 (s, 6H, backbone-Me for [Me₂NN]Cu(η²-ONPh)), 1.433 (s, 6H, [Me₂NN]Cu(benzene)). ¹³C{¹H} NMR (C₆D₆): δ 163.28, 162.44, 160.50, 160.39, 150.62, 147.86, 132.18, 130.63, 129.36, 128.60, 128.24, 125.12, 123.16, 120.13, 95.88, 93.11, 23.15, 22.54, 18.84, 18.52, 14.27. IR: ν_{NO} = 1040 cm⁻¹ (1029 cm⁻¹ for **2b**-¹⁵N). UV-vis (Et₂O): λ_{max} = 580 nm (ε = 2100 M⁻¹ cm⁻¹), 781 nm (ε = 3300 M⁻¹ cm⁻¹). Anal. Calcd for C₄₈H₅₅Cu₂N₅O: C, 68.22; H, 6.56; N, 8.29. Found: C, 67.87; H, 6.78; N, 8.33.

The UV-vis molar absorptivities are approximate: the higher-energy band at λ = 580 nm corresponds to [Me₂NN]Cu(η²-ONAr) (**3b**) from dissociation of a [Me₂NN]Cu fragment in dilute solution.

[Me₂NN]Cu(η²-ONAr) (3a). A solution of ArNO (0.067 g, 0.49 mmol) in ether (5 mL) was slowly added to a solution of [Me₂NN]Cu(MeCN) (0.204 g, 0.49 mmol) in ether (15 mL). The solution turned greenish-black immediately and was allowed to stir

(44) Wiencko, H. L.; Kogut, E.; Warren, T. H. *Inorg. Chim. Acta* **2003**, *345*, 199–208.

for 30 min at room temperature. The solution was then filtered through Celite, and the filtrate was concentrated and cooled to -35 °C. The mauve crystals were isolated from the solution, washed with cold pentane, and dried in vacuo, which afforded 0.150 g (60% yield) of the isolated product. ^1H NMR (C_6D_6): δ 7.058 (d, 4H, *m*-Ar-H), 6.974 (t, 2H, *p*-Ar-H), 6.790 (s, 1H, *p*-ArNO-H), 6.587 (s, 2H, *o*-ArNO-H), 4.772 (s, 1H, backbone-CH), 2.161 (br, 12H, *o*-Ar-Me), 2.046 (s, 6H, ArNO-Me), 1.447 (s, 6H, backbone-Me). $^{13}\text{C}\{^1\text{H}\}$ NMR (C_6D_6): 163.25, 160.90, 138.63, 132.09, 129.78, 128.45, 125.00, 118.27, 95.82, 22.48, 21.00, 18.49. UV-vis (Et_2O): $\lambda_{\text{max}} = 583$ nm ($\epsilon = 550 \text{ M}^{-1} \text{ cm}^{-1}$). Anal. Calcd for $\text{C}_{20}\text{H}_{34}\text{N}_3\text{O}_2\text{Cu}$: C, 69.09; H, 6.79; N, 8.33. Found: C, 68.90; H, 6.81; N, 8.24.

^1H NMR (-60 °C, toluene- d_8 , upfield Me region): δ 2.449 (s, 3H, *o*-Ar-Me) 2.398 (s, 6H, two coincident *o*-Ar-Me groups), 2.054 (s, 6H, ArNO-Me), 1.449 (s, 3H, backbone-Me), 1.357 (s, 3H, backbone-Me), 1.287 (s, 3H, *o*-Ar-Me). Coalescence of the two backbone-Me peaks at 1.449 and 1.357 ppm (300 MHz) gave $\Delta G^\ddagger = 11.4(2)$ kcal/mol at $-44(2)$ °C.

[Me₂NN]Cu(η^2 -ONPh) (3b). A solution of nitrosobenzene (0.049 g, 0.49 mmol) in toluene (5 mL) was slowly added with stirring to a solution of [Me₂NN]Cu(MeCN) (0.205 g, 0.49 mmol) in toluene (10 mL). The solution was stirred for 30 min, concentrated to dryness, taken up in pentane (10 mL), and filtered through Celite. The filtrate was concentrated and cooled to -35 °C. The brown crystals were isolated to afford 0.191 g (82% yield) of product. ^1H NMR (C_6D_6 , RT): δ 7.026 (t, 2H, *m*-PhNO-H), 6.838 (d, 2H, *o*-PhNO-H), 6.753 (t, 1H, *p*-PhNO-H), 4.762 (s, 1H, backbone-CH), 2.143 (br, 12H, *o*-Ar-Me), 1.434 (s, 6H, backbone-Me). $^{13}\text{C}\{^1\text{H}\}$ NMR (C_6D_6): δ 163.26, 160.44, 147.86, 132.16, 129.32, 128.57, 125.08, 120.10, 95.89, 95.82, 22.50, 18.48. IR: $\nu_{\text{NO}} = 1113 \text{ cm}^{-1}$ (1093 cm^{-1} for **3b**- ^{15}N). UV-vis (Et_2O): $\lambda_{\text{max}} = 588$ nm ($\epsilon = 1000 \text{ M}^{-1} \text{ cm}^{-1}$). Anal. Calcd for $\text{C}_{27}\text{H}_{30}\text{CuN}_3\text{O}$: C, 68.11; H, 6.35; N, 8.83. Found: C, 68.20; H, 6.61; N, 8.72.

Addition of NO to {[Me₂NN]Ni}₂(μ - η^2 : η^2 -ONAr) (1a) To Form [Me₂NN]Ni(κ^2 -O₂N₂Ar) (4) and [Me₂NN]Ni(NO). With a syringe, NO gas (2.0 mL @ 300 K and 1 atm, 0.078 mmol) was slowly bubbled into a solution of {[Me₂NN]Ni}₂(μ - η^2 : η^2 -ONAr) (0.032 g, 0.037 mmol) in 5 mL of C_6D_6 . The color of the solution changed instantaneously from dark-green to yellow-green. ^1H NMR

analysis of the reaction mixture indicated a 1:1 molar ratio of [Me₂NN]Ni(κ^2 -O₂N₂Ar)³⁰ (**4**) and [Me₂NN]Ni(NO).³⁰ ^1H NMR (C_6D_6): δ 7.192 (d, 4H, *m*-Ar-H, ([Ni]NO)), 7.04–7.00 (m, 8H, *p*-Ar-H ([Ni]NO), all Ar-H [Ni](O₂N₂Ar)), 6.556 (s, 2H, *o*-ArNO-H), 6.410 (s, 1H, *p*-ArNO-H), 4.883 (s, 1H, backbone-CH [Ni](O₂N₂Ar)), 4.351 (s, 1H, backbone-CH ([Ni]NO)), 2.693 (s, 12H, *o*-Ar-Me [Ni](O₂N₂Ar)), 2.568 (s, 12H, *o*-Ar-Me ([Ni]NO)), 1.825 (s, 6H, ArNO-Me [Ni](O₂N₂Ar)), 1.460 (s, 6H, backbone-Me ([Ni]NO)) 1.433 (s, 6H, backbone-Me [Ni](O₂N₂Ar)).

Addition of NO to [Me₂NN]Cu(η^2 -ONAr) (3a) To Form [Me₂NN]Cu(κ^2 -O₂N₂Ar) (5). With a syringe, NO gas (5.7 mL at 300 K and 1 atm., 0.23 mmol) was slowly bubbled into a solution of [Me₂NN]Cu(η^2 -ONAr) (0.056 g, 0.11 mmol) in 5 mL of pentane. The color changed instantaneously from green to red. Volatiles were removed in vacuo, after which the residue was extracted with pentane and the extracts were filtered through Celite. The filtrate was concentrated and cooled to afford 0.046 g (80% yield) of the product. EPR (toluene, RT) $g_{\text{iso}} = 2.10$ ($A_{\text{Cu}} = 79$ G; $A_{\text{N}} = 13$ G). UV-vis (Et_2O): $\lambda_{\text{max}} = 573$ nm ($\epsilon = 450 \text{ M}^{-1} \text{ cm}^{-1}$), 768 nm ($\epsilon = 180 \text{ M}^{-1} \text{ cm}^{-1}$); Anal. Calcd. for $\text{C}_{25}\text{H}_{34}\text{N}_4\text{O}_2\text{Cu}$: C, 65.20; H, 6.41; N, 10.49. Found: C, 64.98; H, 6.44; N, 10.54.

Acknowledgment. T.H.W. thanks Georgetown University for a Pilot Research Grant, the ACS PRF (G and AC), and the NSF (CAREER program and CHE-0716304). We also thank Prof. Jeffrey Petersen for acquiring the EPR spectra of **5**, Prof. Karsten Meyer for SQUID data on **1a**, and Prof. Faye Rubinson and Mr. Anthony Kammerich for assistance with the cyclic voltammetry of **3a**.

Supporting Information Available: Synthetic details for the ^{15}N -labeled adducts (**1b**–**3b**); additional characterization data for compounds **1**–**5**, including NMR, EPR, and IR spectra; cyclic voltammetry of **3a**; DFT calculational details for **1a**; and X-ray data (CIF) and fully labeled ORTEP plots for **1a**, **2a**, **2b**, **3a**, **3b**, and **5**. This material is available free of charge via the Internet at <http://pubs.acs.org>.

JA903550N